SCIENCE CHINA PRESS

SCIENCE CHINA Life Sciences
life.scichina.com link.springer.com
https://doi.org/10.1007/s11427-024-2698-6

RESEARCH PAPER

BEND6 promotes RNA viruses' replication by inhibiting innate immune responses

Tong Chen[1†], Ling Ding[1†], Shaoyu Tu[1], Huimin Sun[1], Jiahui Zou[1], Aotian Ouyang[1], Meijun Jiang[1], Yi Feng[1], Meilin Jin[1,4], Huanchun Chen[1,2,3,4] & Hongbo Zhou[1,2,3,4*]

[1]National Key Laboratory of Agricultural Microbiology, College of Veterinary Medicine, Huazhong Agricultural University, Wuhan 430070, China
[2]Frontiers Science Center for Animal Breeding and Sustainable Production, Wuhan 430070, China
[3]Hubei Hongshan Laboratory, Wuhan 430070, China
[4]Key Laboratory of Preventive Veterinary Medicine in Hubei Province, The Cooperative Innovation Center for Sustainable Pig Production, Wuhan 430070, China

†Contributed equally to this work
*Corresponding author (email: hbzhou@mail.hzau.edu.cn)

Received 26 March 2024; Accepted 28 July 2024; Published online 10 January 2025

Innate immunity serves as a crucial defense mechanism against invading pathogens, yet its negative regulatory network remains under explored. In this study, we identify BEN domain-containing protein 6 (BEND6) as a novel negative regulator of innate immunity through a genome-scale CRISPR knockout screen for host factors essential for viral replication. We show that BEND6 exhibits characteristics of an interferon-stimulated gene (ISG), with its mRNA and protein levels upregulated by RNA virus-induced IFN-β. BEND6 targets IRF3 and inhibits its recruitment by TBK1, thus preventing IRF3 phosphorylation and dimerization. Additionally, BEND6 directly binds to ISRE, thereby hindering the DNA binding activity of IRF3 and blocking the subsequent activation of IFN-β transcription. Taken together, our study reveals the mechanism of BEND6 in promoting the replication of various RNA viruses and provides a potential therapeutic target for RNA virus infection.

innate immunity | BEND6 | RNA virus | IRF3 | IFN-β

INTRODUCTION

RNA viruses are a diverse group of viruses that use RNA (ribonucleic acid) instead of DNA (deoxyribonucleic acid) as their genetic material (Fairman et al., 2021). Their varied nature enables them to cause a wide range of diseases in humans, animals, and plants, making them of significant interest in virology and infectious disease research (Wang et al., 2024; Zhang et al., 2022). The illnesses caused by RNA viruses range from mild, such as seasonal influenza (caused by influenza A and B viruses), to severe and life-threatening diseases like Ebola (Ebola virus), AIDS (Human Immunodeficiency Virus), and COVID-19 (SARS-CoV-2) (Nakagawa et al., 2023). The rapid mutation rates lead to considerable genetic viabilities of RNA viruses, which pose significant challenges for vaccine and treatment development. All RNA viruses require the cellular machineries of their hosts for proliferation (Zhu et al., 2023). Throughout the ongoing evolutionary struggle between viruses and their hosts, the hosts have developed complex defense mechanisms, while viruses have continuously adapted to these defenses.

The innate immune system serves as the host's first line of defense against invading pathogens. Activation of innate immunity requires the recognition of pathogens by pathogen recognition receptors (PRRs), including Toll-like receptors (TLRs), C-type lectin receptors (CLRs), NOD-like receptors (NLRs), and RIG-I-like receptors (RLRs) (Rivera et al., 2016; Wang and Chai, 2020). Among these receptors, RLRs play a crucial role in recognizing RNA viruses and activating the downstream MAVS-IKK/TBK1 signal cascades. Amid this signal transduction pathway, TBK1 recruits and phosphorylates IRF3, which leads to its dimerization and nuclear import. Once in the nucleus, IRF3 binds to interferon-stimulated response elements (ISREs), and ultimately triggers the expression and secretion of Type I interferons (IFN-I) (Rivera et al., 2016).

Our previous study employed a genome-scale CRISPR knockout library to identify host factors essential for influenza A virus (IAV) replication in newborn pig trachea (NPTr) cells, which revealed BEN domain-containing protein 6 (BEND6) as a top-ranked candidate (data not shown). Current knowledge about BEND6 is limited. It was reported that BEND6 assists the Notch signaling pathway to regulate intracellular transcription and to maintain intracellular homeostasis (Abhiman et al., 2008). The BEN domain of BEND6 interacts with CBF1, the core component of the Notch signaling pathway, thereby inhibiting the transduction of Notch signals (Duan et al., 2011). However, despite its known involvement in the Notch signaling pathway, the virus-related functions of BEND6 necessitates further investigation.

Citation: Chen, T., Ding, L., Tu, S., Sun, H., Zou, J., Ouyang, A., Jiang, M., Feng, Y., Jin, M., Chen, H., et al. BEND6 promotes RNA viruses' replication by inhibiting innate immune responses. Sci China Life Sci, https://doi.org/10.1007/s11427-024-2698-6

In this study, we show that BEND6 promotes the replication of multiple RNA viruses by targeting the innate immune signaling pathway. Mechanistically, BEND6 suppresses the phosphorylation and dimerization of IRF3 by inhibiting the recruitment of IRF3 by TBK1, thereby preventing the nucleus entry of IRF3. Additionally, the direct binding of BEND6 to ISRE impairs the DNA-binding activity of IRF3. Our study reveals a novel function of BEND6 as a negative regulator of innate immunity and provides a therapeutic target for combating viral infections.

RESULTS

BEND6 promotes the replication of multiple RNA viruses

Given that the relationship between BEND6 and IAV has never been previously reported, we examined the effects of BEND6 on the proliferation of IAV. Prior to this, we generated BEND6 knockout (KO) cells using CRISPR/Cas9 technique in wild type (WT) PK15 cells. KO efficiency was validated by Sanger sequencing, which revealed a 5-base deletion in BEND6-KO cells (Figure S1A in Supporting Information). Meanwhile, we confirmed that knocking out BEND6 had no significant effect on cell viability (Figure S1B in Supporting Information). Due to the lack of commercial BEND6 antibody, we generated polyclonal antibody in mice using purified BEND6-His protein. The specificity of the antibody was validated through enzyme-linked immunosorbent assays (ELISA) and indirect immunofluorescence assays, with serum of untreated mice as the negative control. As shown in Figure S1C and D in Supporting Information, strong reactivity of the BEND6 polyclonal antibody to BEND6-His protein and PK-15 cells can be observed, which indicates high specificity of the antibody. Subsequently, this antibody was used to detect the knockout efficiency of BEND6 KO cells by western blot. The results confirmed the significant reduction in BEND6 protein level in BEND6 KO cells compared with that of WT PK15 cells (Figure S1E in Supporting Information). To assess the impact of BEND6 on IAV replication, BEND6 KO and WT PK15 cells were infected with equivalent doses of swine influenza virus HB/H1N1 and F26/H1N1, human influenza virus PR8/H1N1 or avian influenza virus 115/H9N2. The results showed that knockout of BEND6 significantly decreased the release of infectious virus particles and intracellular NP levels of various IAV subtypes at 12, 24, and 36 h post-infection (hpi) (Figure 1A–D). We further confirmed that this impact was not due to off-target effect, as complementation with a synonymous mutant Flag-BEND6 plasmid (Flag-BEND6 (T)) in BEND6 KO cells increased IAV titers compared with the empty vector group (Figure 1E). Meanwhile, ectopic expression of BEND6 in WT PK15 cells significantly elevated the release of HB/H1N1 virus, and intracellular levels of NP at 24 hpi (Figure 1F).

To explore whether the effect of BEND6 on viral replication extends beyond IAV, we next examined the impact of BEND6 on the proliferation of other RNA viruses. In contrast to IAVs, vesicular stomatitis virus (VSV), Japanese encephalitis virus (JEV) and Sendai virus (SeV) replicate their genomes in the cytoplasm. Using JEV, SeV, and a recombinant VSV-green fluorescent protein (GFP) as models, we found significantly lower levels of VSV and JEV viral proteins and SeV viral mRNA levels in BEND6 KO cells compared with that of WT PK15 cells at 24 hpi (Figure 1G–I). Conversely, complementation with BEND6 expression in PK15 WT cells significantly increased the replication of VSV, JEV, and SeV (Figure 1J–L). Taken together, these data demonstrate that BEND6 is a positive regulator for multiple RNA viruses, which suggests a potential role for BEND6 in antiviral innate immunity.

Virus-induced IFN-β increases the protein and mRNA levels of BEND6

Considering that BEND6 affects the proliferation of a variety of viruses, we next explored the role of BEND6 in IFN-β signaling pathways. The endogenous protein and mRNA levels of BEND6 were determined by western blot and quantitative reverse transcription-PCR (qRT-PCR) upon virus infection. The results showed that the mRNA and protein levels of BEND6 were progressively increased over the time course of IAV infection (Figure 2A and B). Similarly, the increases in BEND6 protein and mRNA levels were also observed after infection with SeV (Figure 2C–E) or VSV-GFP (Figure 2F–H).

To determine whether the increase in BEND6 expression was due to IFN-β induction or viral replication, we examined the BEND6 levels in NPTr cells after stimulated with polyinosinic-polycytidylic acid (poly(I:C)). The results revealed that poly(I:C) stimulation also resulted in an increase in the protein and mRNA levels of BEND6 (Figure 2I–K). Furthermore, PK15 cells treated with varying doses of IFN-β showed a significant upregulation of BEND6 protein and mRNA levels (Figure 2L–N), which indicates that BEND6 expression is induced by IFN-β. Collectively, these findings suggest that virus-induced IFN-β increases BEND6 expression, highlighting a potential role for BEND6 in the IFN-β signaling pathway.

BEND6 negatively regulates the antiviral innate immune responses

To explore the role of BEND6 in the innate immune responses, we first examined its effects on SeV-induced activation of the IFN-β and ISRE promoter. HEK293T cells were co-transfected with swine IFN-β-luc or ISRE-luc, pRL-TK, and Flag-BEND6. Subsequently, the cells were stimulated with SeV, and dual-luciferase reporter assays were performed to measure IFN-β or ISRE-luc promoter activities. The results demonstrated that overexpression of BEND6 significantly inhibited both IFN-β and ISRE promoter activities in a dose-dependent manner (Figure 3A and B). Similarly, overexpression of BEND6 also inhibited the promoter activity of IFN-β or ISRE stimulated by poly(I:C) in a dose-dependent manner (Figure 3C and D). Additionally, we examined the effects of BEND6 on the transcription of swine IFN-β and downstream interferon-stimulated genes (ISGs), including *ISG15*, *ISG54*, *OAS1*, and *Mx1*, after viral infection. BEND6 KO cells and WT PK15 cells were infected with HB/H1N1 or SeV, and the mRNA levels of above-mentioned genes were detected by qRT-PCR. The results indicated that knocking out of BEND6 significantly increased the mRNA levels of IFN-β and ISGs under the IAV and SeV infection (Figure 3E and F).

BEND6 negatively regulates IFN-β signal pathway by targeting IRF3 signaling

It is widely acknowledged that RNA viruses are recognized by RIG-I, which subsequently initiates a signal transduction cascade involving MAVS, TBK1/IKK, and IRF3 and ultimately leads to

https://doi.org/10.1007/s11427-024-2698-6

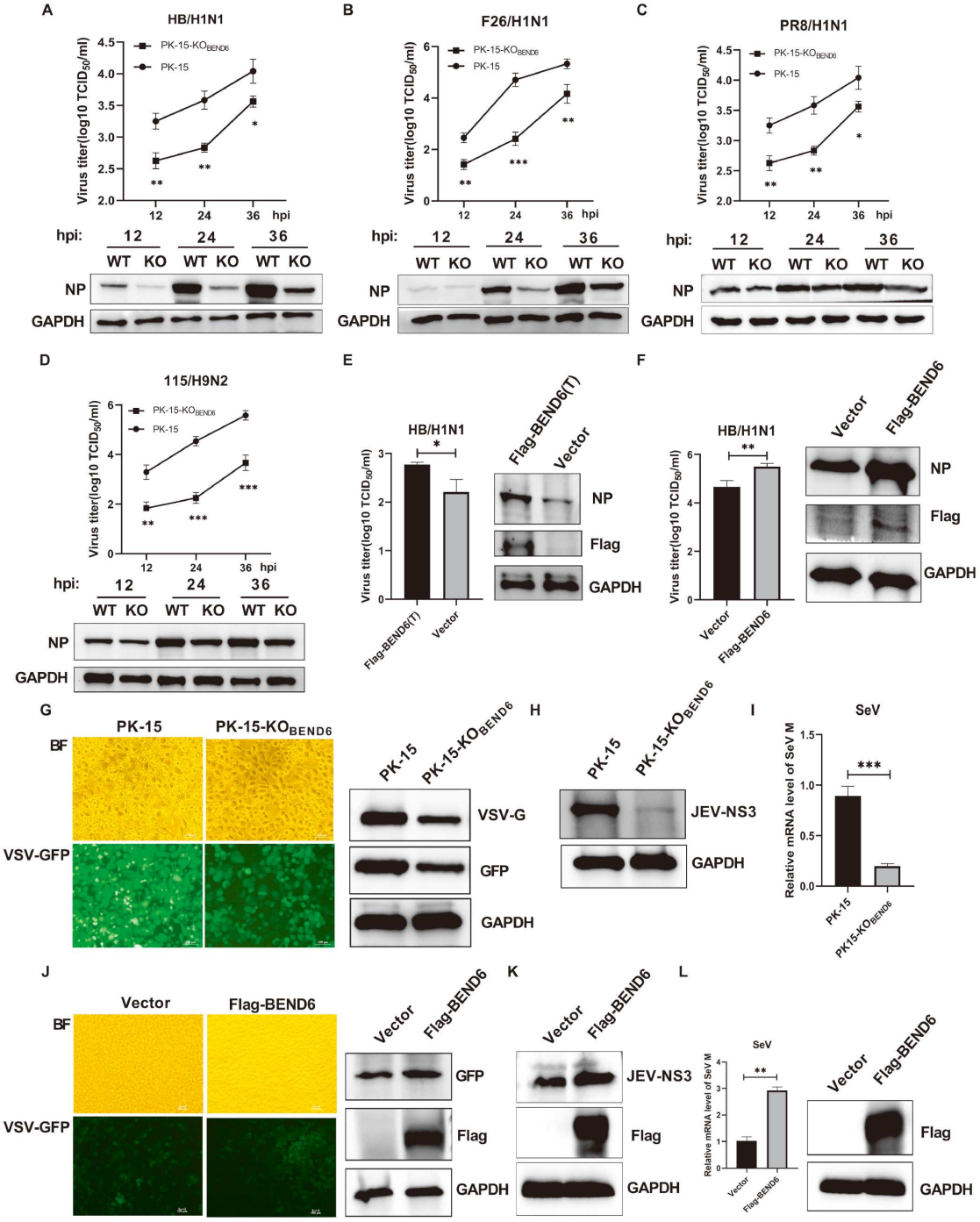

Figure 1. BEND6 promotes the replication of multiple RNA viruses. A–D, BEND6 KO and WT PK15 cells were infected with HB/H1N1 virus, F26/H1N1 virus, PR8/H1N1 virus or 115/H9N2 virus at a multiplicity of infection (MOI) of 0.01. At 12, 24, 36 hpi, viral NP protein levels were examined by western blot, and GAPDH served as a loading control. Viral titers in the supernatants were determined by $TCID_{50}$ assay on MDCK cells. E, BEND6 KO cells or F, WT PK15 cells were transfected with (E) Flag-BEND6 synonymous mutation plasmid or empty vector and (F) Flag-BEND6 or empty vector for 24 h, respectively, followed by infection with HB/H1N1 virus (MOI, 0.1). At 24 hpi, NP and Flag-BEND6 proteins levels were examined by western blot, GAPDH served as a loading control, and viral titers in the supernatants were determined by $TCID_{50}$ assay on MDCK cells. G, BEND6 KO and WT PK15 cells were infected with VSV-GFP (MOI, 1.0). Samples were collected at 24 hpi. The VSV-GFP was visualized by fluorescence microscopy, scale bar = 100 μm, VSV viral protein levels were examined by western blot, and GAPDH served as a loading control. H, BEND6 KO and WT PK15 cells were infected with JEV (MOI, 0.5). JEV NS3 protein levels were examined by western blot at 24 hpi, and GAPDH served as a loading control. I, BEND6 KO and WT PK15 cells were infected with SeV (MOI, 1.0). The mRNA level of SeV-M was detected by qRT-PCR, and the viral RNAs levels were normalized to the GAPDH level. J, HEK293T cells were transfected with Flag-BEND6 or empty vector for 24 h, followed by infection with VSV-GFP (MOI, 1.0). Samples were collected at 24 hpi. The VSV-GFP was visualized by fluorescence microscopy, scale bar = 100 μm, VSV viral protein levels were examined by western blot, and GAPDH served as a loading control. K, HEK293T cells were transfected with Flag-BEND6 or empty vector for 24 h, followed by infection with JEV (MOI, 10), JEV NS3 and Flag-BEND6 protein levels were examined by western blot at 24 hpi, and GAPDH served as a loading control. L, HEK293T cells were transfected with Flag-BEND6 or empty vector for 24 h, the mRNA levels of SeV-M were detected by qRT-PCR, and the viral RNAs levels were normalized to the GAPDH level. Flag-BEND6 protein levels were examined by western blot at 24 hpi, and GAPDH served as a loading control (means±SD from three independent experiments) (*, $P<0.05$; **, $P<0.01$; ***, $P<0.001$; all by two-tailed Student's t test).

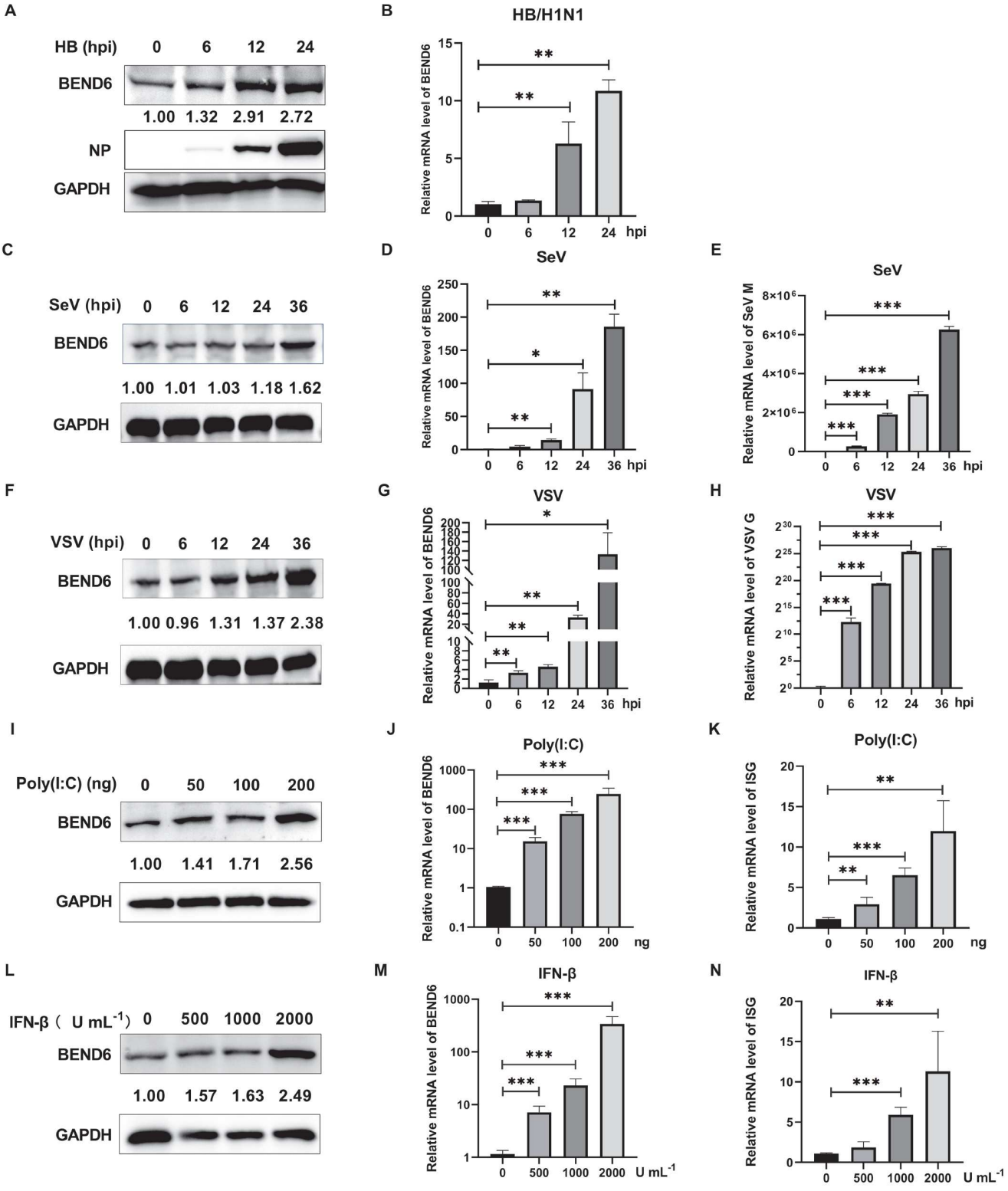

Figure 2. Virus-induced IFN-β increases the protein and mRNA levels of BEND6. A and B, PK15 cells were infected with HB/H1N1 (MOI, 0.1). At 0, 6, 12, 24 hpi, endogenous BEND6 and viral NP protein levels were examined by western blot, and the mRNA levels of BEND6 were detected by qRT-PCR. C–E, PK15 cells were infected with SeV (MOI, 1.0). At 0, 6, 12, 24, 36 hpi, endogenous BEND6 protein levels were examined by western blot, and the mRNA levels of BEND6 and SeV-M were detected by qRT-PCR. F–H, PK15 cells were infected with VSV (MOI, 1.0). At 0, 6, 12, 24, 36 hpi, endogenous BEND6 protein levels were examined by western blot, and the mRNA levels of BEND6 and VSV-G were detected by qRT-PCR. I–K, NPTr cells were transfected with 0, 50, 100, 200 ng poly(I:C) for 12 h. The endogenous BEND6 protein levels were examined by western blot, and the mRNA levels of BEND6 and ISG15 were detected by qRT-PCR. L–N, PK15 cells were treated with increasing concentrations of human IFN-β (0, 500, 1,000, and 2,000 U mL^{-1}) for 12 h, The endogenous BEND6 protein levels were examined by western blot, and the mRNA levels of BEND6 and ISG15 were detected by qRT-PCR. The above proteins and mRNA levels detection all used GAPDH as an internal reference (means±SD from three independent experiments) (*, P<0.05; **, P<0.01; ***, P<0.001; all by two-tailed Student's t test).

https://doi.org/10.1007/s11427-024-2698-6

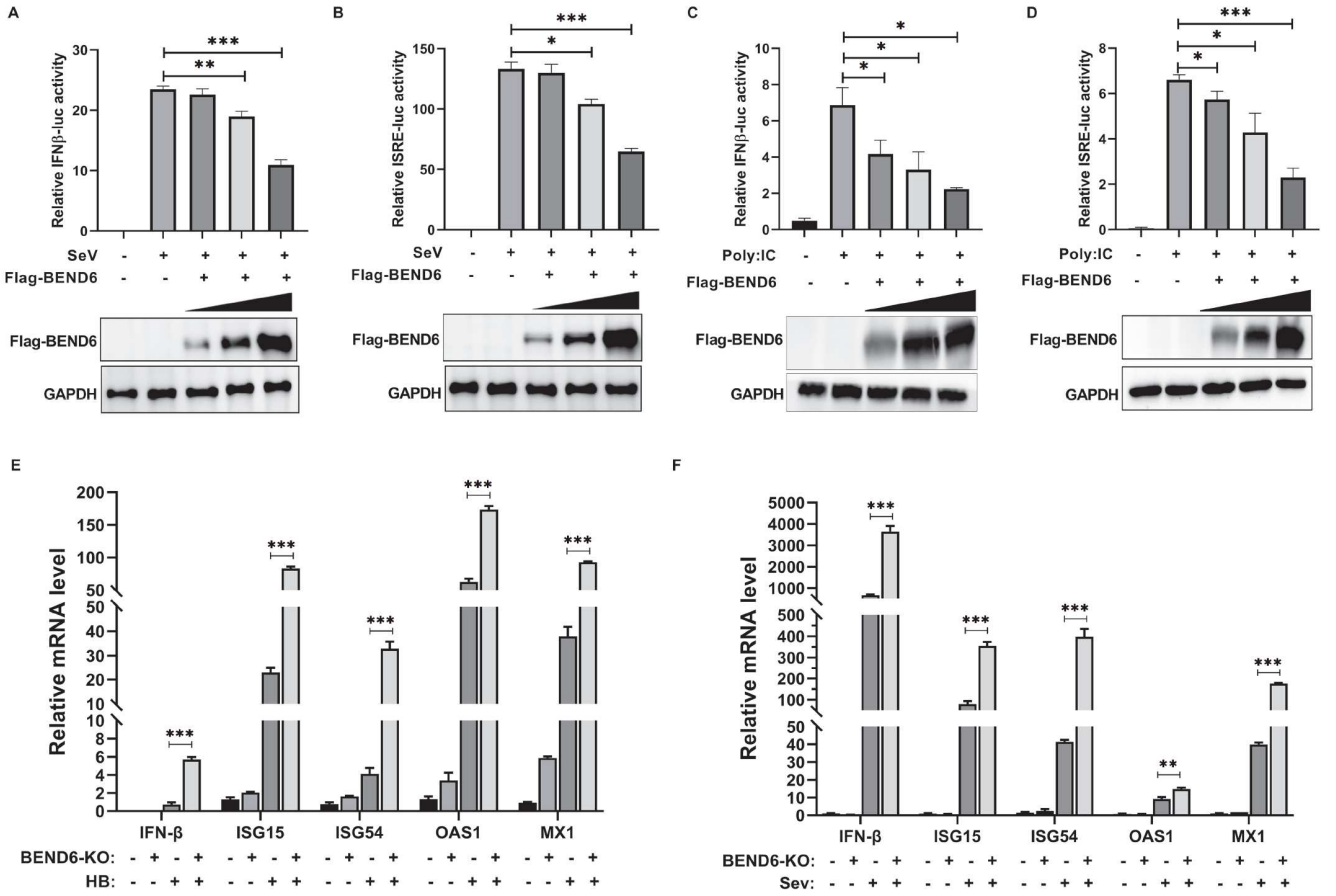

Figure 3. BEND6 negatively regulates the antiviral innate immune responses. A and B, HEK293T cells were co-transfected with swine IFN-β-luc or ISRE-luc, pRL-TK, and Flag-BEND6 for 24 h. Then, cells were stimulated with SeV for 12 h, and dual-luciferase reporter assays were performed to measure IFN-β or ISRE-luc promoter activity. C and D, HEK293T cells were co-transfected with swine IFN-β-luc or ISRE-luc, pRL-TK, and Flag-BEND6 for 24 h, then cells were transfected with 100 ng poly(I:C) for 12 h, and dual-luciferase reporter assays were performed to measure IFN-β or ISRE-luc promoter activity. E and F, BEND6 KO and WT PK15 cells were infected with HB/H1N1 (MOI, 0.1) or SeV (MOI, 1.0) for 24 h, then the mRNA levels of IFN-β, ISG15, ISG54, OAS1 and MX1 were detected by qRT-PCR, and the mRNAs levels were normalized to the GAPDH level (means±SD from three independent experiments) (*, $P<0.05$; **, $P<0.01$; ***, $P<0.001$; all by two-tailed Student's t test).

the transcription of IFN-β (Kell and Gale, 2015). Therefore, we next explored the specific target of BEND6 in the negative regulation of IFN signaling pathway. Swine IFN-β-luc or ISRE-luc, pRL-TK, Flag-BEND6 and different interferon signaling molecules (including swine RIG-I, MAVS, TBK1/IKK, or IRF3) were co-transfected in HEK293T cells, and dual-luciferase reporter assays were performed to measure IFN-β-luc promoter activity after 24 h. The results showed that BEND6 significantly reduced IFN-β promoter activity activated by these IFN signaling molecules (Figure 4A–E). Given these findings, we hypothesized that BEND6 might target IRF3. To investigate this, co-inmunoprecipitation (co-IP) assays were conducted to assess the interaction of IRF3 and BEND6. The results showed that exogenous BEND6 strongly interacted with exogenous IRF3 in HEK293T cells under SeV infection (Figure 4F and G). Additionally, endogenous BEND6 also interacted with endogenous IRF3 in PK15 cells under SeV infection (Figure 4H). Collectively, the results indicate that BEND6 negatively regulates the IFN-β signaling pathway by targeting IRF3.

BEND6 inhibits the recruitment of TBK1 to IRF3

Upon viral infection, TBK1 recruits IRF3 to facilitate IRF3 phosphorylation, leading to its dimerization and nuclear translocation to activate IFN-β gene transcription (Kell and Gale, 2015; Yang et al., 2019). To explore the mechanism by which BEND6 targets IRF3 to inhibit the innate immune signaling pathway, we first examined whether BEND6 affects the recruitment of IRF3 by TBK1. We found that increasing levels of BEND6 progressively weakened the interaction between IRF3 and TBK1 (Figure 5A). Previous studies have shown that TBK1 directly phosphorylates two groups of amino acid residues (Group I: serines 385 and 386 and Group II: the serine/threonine cluster between amino acids 396 and 405) at the C-terminal of IRF3 (Fitzgerald et al., 2003; McWhirter et al., 2004; Sharma et al., 2003). Therefore, to investigate the mechanism of how BEND6 weakens the TBK1-IRF3 interaction, we constructed a truncated IRF3 (380-427aa, FLAG-GFP-λIRF3) containing Group I and Group II (McWhirter et al., 2004). The truncated IRF3 was used to determine whether the domain of IRF3 that binds to BEND6 is the same as that bound by TBK1. Co-IP experiments results showed that BEND6 and TBK1 compete to bind to the same region of IRF3 (Figure 5B and C). To further confirm our results, we examined the effects of BEND6 on IRF3 phosphorylation and dimerization. The results showed that overexpression of BEND6 reduced the phosphorylation level of IRF3 (Figure 5D) and

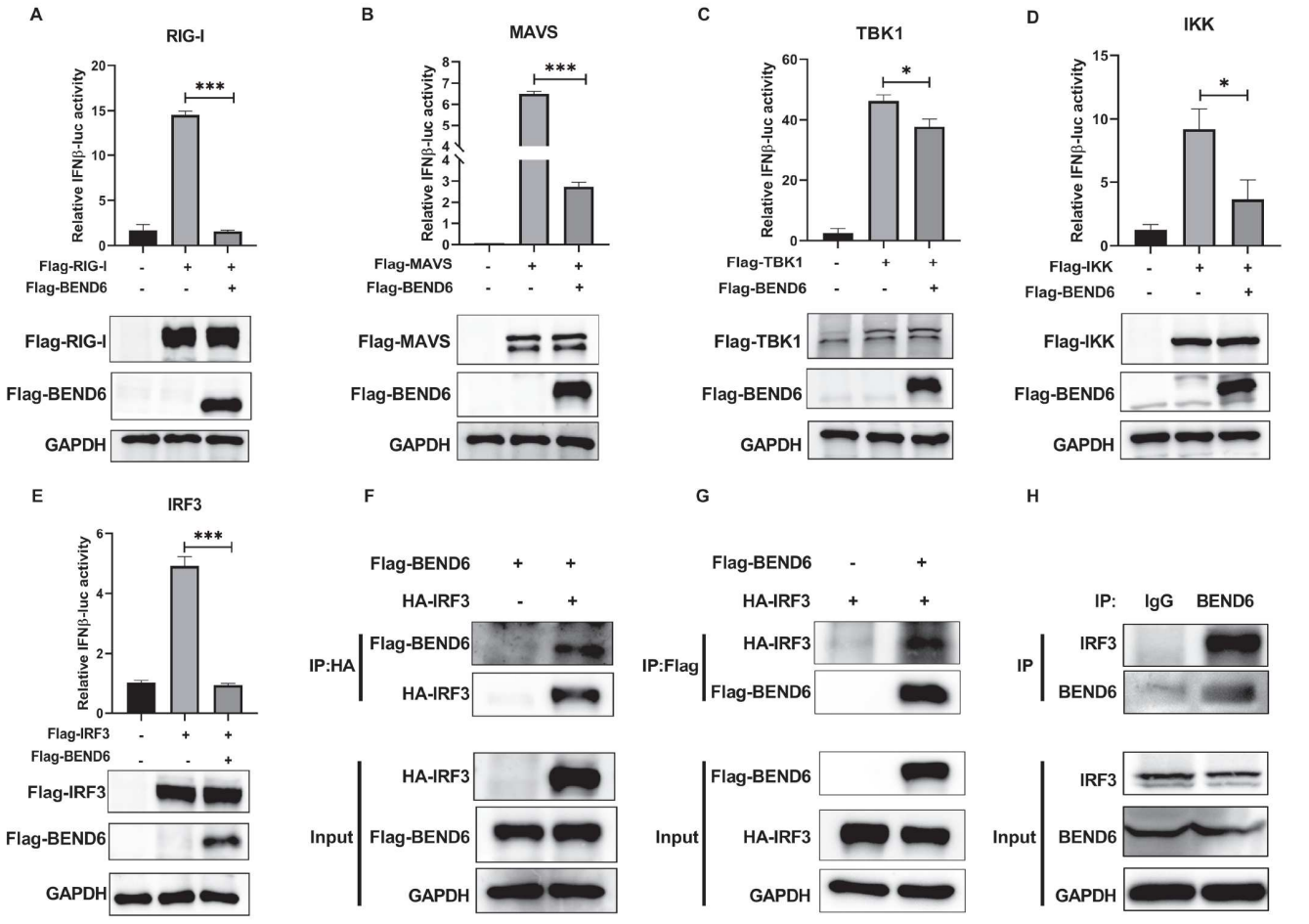

Figure 4. BEND6 negatively regulates IFN-β signal pathway by targeting IRF3 signaling. A–E, HEK293T cells were co-transfected with Swine IFN-β-luc or ISRE-luc, pRL-TK, Flag-BEND6 and different interferon signaling molecules (swine RIG-I, MAVS, TBK1/IKK or IRF3) for 24 h, dual-luciferase reporter assays were performed to measure IFN-β-luc promoter activity, the protein levels of Flag-BEND6 and interferon signaling molecules were detected by western-blot, and GAPDH served as a loading control (means±SD from three independent experiments) (*, $P<0.05$; **, $P<0.01$; ***, $P<0.001$; all by two-tailed Student's t test). F and G, HEK293T cells were co-transfected with the Flag-BEND6, HA-IRF3 and indicated empty vector for 24 h. Co-IP was performed using either (F) anti-HA or (G) anti-Flag antibody, followed by western blot. H, The co-purification between endogenous BEND6 and IRF3. Co-IP was performed using an anti-BEND6 mouse antibody or mouse IgG with SeV infection. The endogenous BEND6 and coprecipitated IRF3 were detected using an anti-BEND6 antibody and an anti-IRF3 antibody, respectively. Mouse IgG was used as the negative control.

impaired IRF3 dimerization (Figure 5E). The effect of BEND6 on IRF3 dimerization was also determined by a native polyacrylamide gel electrophoresis (PAGE) assay, in which HA-IRF3 was co-transfected with increasing amounts of Flag-BEND6 in HEK293T cells. The results revealed that the IRF3 dimerization was impaired when BEND6 was overexpressed (Figure 5F). Taken together, these results indicate that BEND6 inhibits the recruitment of IRF3 by TBK1 to reduce the phosphorylation and dimerization of IRF3, thereby negatively regulating innate immune response.

The BEN domain is the main domain of BEND6 that is crucial for its biological functions. To further investigate the specific regions of BEND6 that mediate the BEND6-IRF3 interaction, we attempted to truncate BEND6 based on the BEN domain. However, the truncated BEND6 lacking 170 amino acids at the N-terminal failed to express any proteins. Thus we constructed three truncated BEND6: N170 (1–170 aa, N- terminal), N271 (1–271 aa, N- terminal), and the ΔBEN domain (1–170 and 272–279 aa) (Figure S2A in Supporting Information). Co-IP results showed that IRF3 only interacted with the full-length BEND6, indicating that the BEND6-IRF3 interaction requires not only the BEN domain of BEND6 (Figure S2B in Supporting Information).

BEND6 impairs the DNA binding ability of IRF3

As a transcriptional regulator, BEND6 is distributed in both the cytoplasm and nucleus, while IRF3 binds to the ISREs sequence to activate the transcription of target genes (Weaver et al., 1998). Therefore we investigated whether its interaction with IRF3 affects the ability of IRF3 to bind to DNA. HEK293T cells were co-transfected with Flag-BEND6, Flag-IRF3, or the corresponding empty vector. After 24 h, the cells were infected with SeV for 12 h. A DNA pulldown assay was then performed using a biotinylated ISRE or unbiotinylated ISRE as the probe to detect IRF3 binding to ISRE oligonucleotides. The results showed that the amounts of Flag-IRF3 pulled down by the biotin-ISRE gradually increased with increasing ISRE probe, while no Flag-IRF3 protein was pulled down by unbiotinylated ISRE. However, in the presence of BEND6, the levels of Flag-IRF3 pulled down by

https://doi.org/10.1007/s11427-024-2698-6

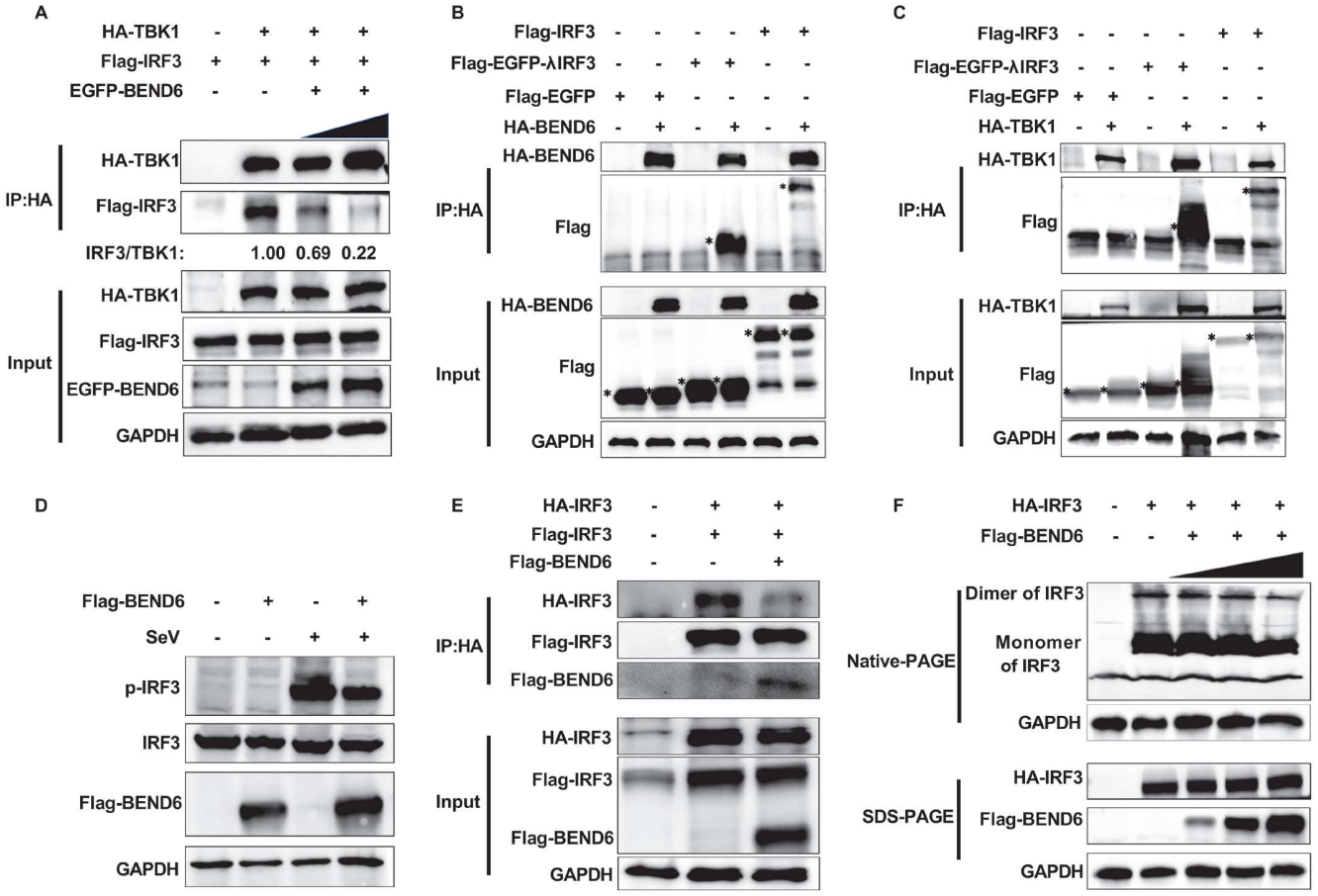

Figure 5. BEND6 inhibits the recruitment of TBK1 to IRF3. A, HEK293T cells were co-transfected with swine Flag-TBK1, HA-IRF3, EGFP-BEND6 and indicated empty vector for 24 h. Co-IP was performed using an anti-Flag antibody, followed by western blot to detect the expression of the plasmids and coprecipitated proteins. The relative band intensities were quantified by Image J. B and C, HEK293T cells were co-transfected with swine Flag-IRF3, Flag-EGFP-λIRF3, Flag-EGFP and HA-BEND6 or HA-TBK1 for 24 h. Co-IP was performed using an anti-HA antibody, followed by western blot to detect the expression and coprecipitation of corresponding proteins. * represents the indicated protein. D, HEK293T cells were transfected with swine Flag-BEND6 for 24 h, followed by infection with or without SeV for 12 h, indicated protein levels were detected by western blot, and GAPDH served as a loading control. E, HEK293T cells were co-transfected with swine Flag-IRF3, HA-IRF3, Flag-BEND6 and indicated empty vector, Co-IP was performed using an anti-HA antibody, followed by western blot to detect the expression and coprecipitation of corresponding proteins, and GAPDH served as a loading control. F, HEK293T cells were co-transfected with swine HA-IRF3, Flag-BEND6 and indicated empty vector. The IRF3 dimer was detected by native PAGE analysis.

biotin-ISRE were significantly reduced compared with that of the control group (Figure 6A). This indicates that BEND6 affects IRF3's binding to ISRE, potentially due to its interaction with IRF3 or direct binding to ISRE, as recent research shows BEND6 can bind DNA (Liu et al., 2023). To verify this, we purified the prokaryotic BEND6-His protein and 4M2e-His protein (which served as a negative control), and directly incubated them with biotinylated ISRE or unbiotinylated ISRE in equal amounts. The results showed that BEND6 was significantly pulled down by biotin-ISRE compared with the negative control group, which indicates the direct interaction of BEND6 with ISRE (Figure 6B). These findings suggest that BEND6 impairs IRF3 binding to ISRE by interacting with both IRF3 and ISRE, thereby negatively regulating IFN-β transcription.

DISCUSSION

Host factors play a crucial role in the viral life cycle, and the construction of a genome-scale knockout or activation library to screen for essential or restrictive factors of virus proliferation are the key methods for understanding the viral life cycle and pathogenesis (Das et al., 2020; Wei et al., 2021; Wu et al., 2018). This approach provides a molecular basis for developing novel antiviral strategies beyond vaccines, such as antiviral drugs targeting host factors or genetically edited animals. Our laboratory utilized a genome-scale CRISPR knockout library to identify essential host factors for IAV replication in porcine NPTr cells, with BEND6 being the top-ranked candidate (Data not shown). We found that knockout of BEND6 had no negative effect on the cell viability of PK15, and inhibited the proliferation of various RNA viruses by promoting innate immune responses. This suggests that BEND6 could serve as a potential target for broad-spectrum antiviral drugs and the breeding genetically edited pigs that are resistant to multiple viral infections.

Our study found that the mRNA and protein levels of BEND6 significantly increased upon various viral infections, poly(I:C), and IFN-β stimulation, indicating that BEND6 possesses characteristics of ISGs. While most ISGs play antiviral roles, some IFN-induced genes also exhibit pro-viral activity. For example, the IFN-inducible gene LY6E promotes HIV, type 1 (HIV-1) infection by enhancing viral entry and gene expression (Yu et al., 2017). Meanwhile, as a classic ISG, OASL was shown to promote

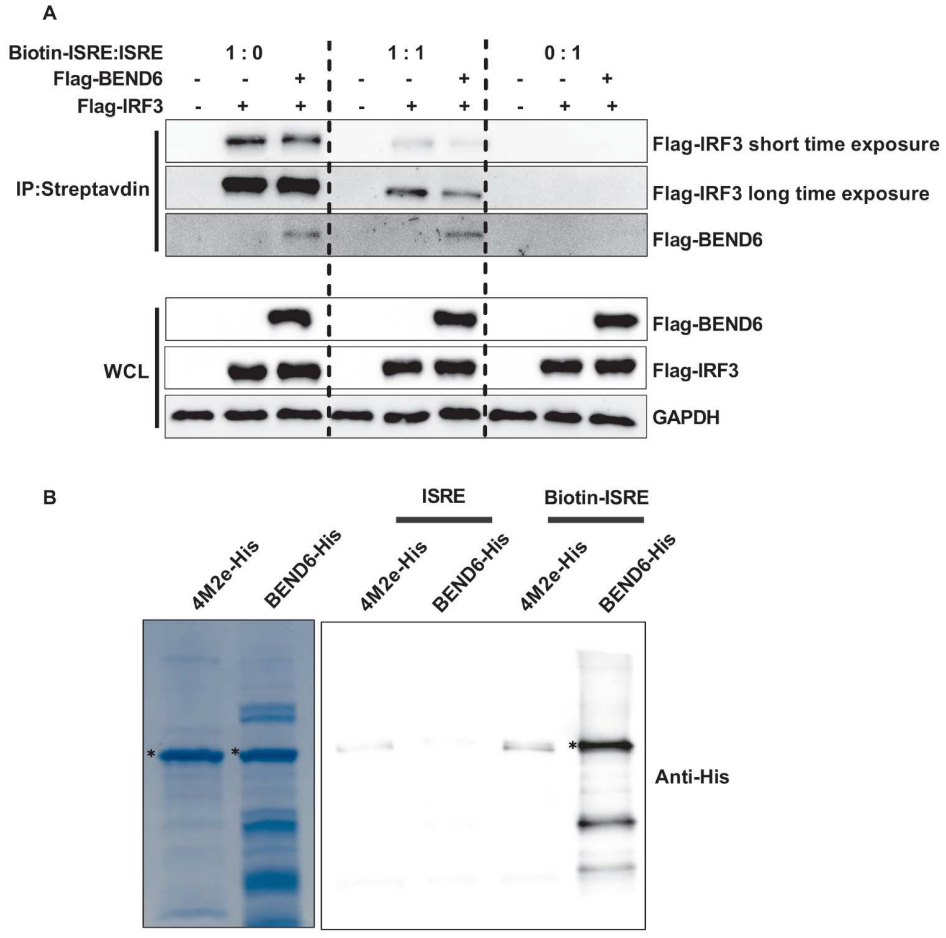

Figure 6. BEND6 impairs the DNA binding ability of IRF3. A, HEK293T cells were co-transfected with Flag-BEND6, Flag-IRF3 and the corresponding empty vector for 24 h, followed by infection with SeV (MOI, 10) for 12 h. Then, the DNA pulldown assay was carried out to detect the amount of IRF3 bound to ISRE oligonucleotide by using a biotinylated ISRE or unbiotinylated ISRE as the probe, followed by western blot to detect the expression and coprecipitation of corresponding proteins. B, Equal amounts of BEND6-His protein and 4M2e-His protein (10 μg) were used for DNA pulldown assay with ISRE, followed by western blot to detect coprecipitation of corresponding proteins (right), and the protein level and purity of BEND6-His protein and 4M2e-His protein assessed by Coomassie brilliant blue staining (left). * represents the indicated protein.

infection by interaction with the ORF20 protein of Kaposi's sarcoma-associated herpesvirus (KSHV) (Bussey et al., 2018). Similar genes include USP18 (Lai et al., 2023), ADAR1 (Gélinas et al., 2011), IFN-γ-inducible protein 10 (IP-10) (Wang et al., 2017), and CD169 (Akiyama et al., 2017). These examples show that viruses, through evolution and long-term interaction with hosts, can adapt to and manipulate host factors for their own benefit. However, the precise mechanisms of how IFN-β induces the mRNA and protein levels of BEND6 remain to be investigated.

BEND6 negatively regulates the Notch signaling pathway transcription through two mechanisms: the BEN domain of BEND6 binds to CBF1, thereby inhibiting the recruitment of p300/CPB by CBF1 and subsequent transcription (Duan et al., 2011), and the BEN domain binds to CGCG DNA sequences or AAA-containing matrix attachment regions (Liu et al., 2023). Our study reports for the first time that BEND6 participated in the regulation of innate immune signaling pathways. Interestingly, BEND6 also regulates the transcription of IFN-β by binding to proteins and DNA. Specifically, BEND6 bound to the same region of IRF3 as TBK1, thereby inhibiting the recruitment of IRF3 by TBK1, as well as the phosphorylation and dimerization of IRF3. Additionally, BEND6 directly binds to ISRE and IRF3 binding to ISRE. The ISRE sequence contains AAA and CGCG DNA sequences, which is consistent with the preference of the BEN domain.

Based on our findings, we propose a model for the negative regulation of BEND6 on innate immune signaling pathway (Figure 7). RNA Virus-induced IFN-β upregulates the expression of BEND6, which binds to IRF3 and inhibits its recruitment by TBK1, thereby impairing the phosphorylation and dimerization of IRF3, and reducing the nuclear entry of IRF3. Simultaneously, BEND6 directly binds to ISRE, hindering the binding of IRF3 to ISRE and reducing the transcription of interferon. In summary, our study reveals the specific mechanism by which BEND6 negatively regulates interferon transcription induced by RNA viruses, which would increase our understanding of the negative regulation of the host innate immunity and the functions of BEND6 in virus replication.

MATERIALS AND METHODS

Cells and viruses

Madin–Darby canine kidney cells (MDCK), Human embryonic kidney 293T cells (HEK293T), newborn pig trachea (NPTr) and Pig kidney cells (PK-15) were purchased from ATCC (American

https://doi.org/10.1007/s11427-024-2698-6

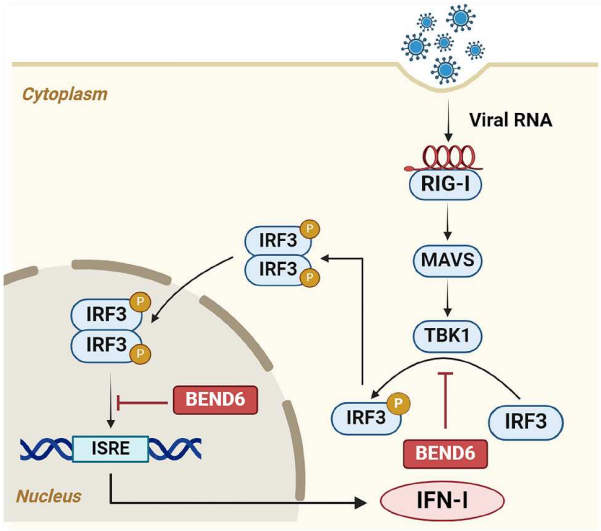

Figure 7. Proposed model for the mechanism of BEND6 inhibits the IFN-β signal pathway. RNA viral infections induce IFN-I production and subsequently increase the mRNA and protein levels of BEND6. BEND6 binds to IRF3 and inhibits the recruitment of IRF3 by TBK1, thereby inhibiting the phosphorylation and dimerization of IRF3, and reducing the nuclear entry of IRF3. On the other hand, BEND6 directly binds to ISRE, hindering the binding of IRF3 to ISRE and suppressing the transcription of IFN-I.

Type Culture Collection, USA). All cells were cultured in Dulbecco's modified Eagle's medium (DMEM) (HyClone, USA) supplemented with 10% heat-inactivated fetal bovine serum (FBS) (PAN-Biotech, Germany), and incubated at 37°C in a humidified 5% CO_2 incubator (Sanyo, Japan).

A/swine/Hubei/221/2016(HB/H1N1), A/chicken/Hubei/115/2016(115/H9N2), A/swine/Henan/F26/2017 (F26/H1N1) and A/Puerto Rico/8-SV14/1934 (PR8/H1N1) viruses were amplified in 10-day-old specific-pathogen-free (SPF) embryonic chicken eggs (Boehringer Ingelheim Vital Biotechnology, Beijing, China) and stored in our laboratory. SeV was amplified using 10-day-old embryonic chicken eggs (Boehringer Ingelheim Vital Biotechnology, Beijing, China). VSV-GFP was a gift from Harbin Veterinary Research Institute (Harbin, China). JEV was kindly provided by Shengbo Cao (Huazhong Agricultural University, Wuhan, China). For *in vitro* infection of IAV, the culture medium was supplemented with 0.25 μg mL^{-1} of L-tosylamide-2-phenylethyl chloromethyl ketone (TPCK)-treated trypsin (Sigma, USA).

Antibodies

The antibodies used and their sources are as follows: rabbit antibodies against HA tag antibody (Biopmk, Wuhan, China); GFP tag antibodies (Biopmk); Flag tag antibody (Proteintech, Wuhan, China); IAV NP antibody (GeneTex, USA); VSV-G antibody (Abcam, UK); IRF3 (Servicebio, Wuhan, China); phosphorylated IRF3 (ABclonal Biotechnology, Wuhan, China); mouse antibodies against glyceraldehyde 3-phosphate dehydrogenase (GAPDH) antibody (Proteintech); horseradish peroxidase (HRP)-conjugated anti-mouse (Beijing Biodragon Inmmunotechnologies, Beijing, China) and anti-rabbit (Beijing Biodragon Inmmunotechnologies). BEND6 protein antibody was generated by our laboratory. JEV-NS3 antibody was gifted by Professor Li Xiangmin from Huazhong Agricultural University.

Plasmids

To construct the HA-BEND6, Flag-BEND6, BEND-GFP and BEND6-His expression plasmids, the coding regions of *BEND6* (XM_001925201) were PCR-amplified from cDNA derived from PK-15 cells and cloned into pCDNA3.4, pCAGGS-HA, p3XFLAG-CMV-14, pEGFP-N1 and PET32a vectors. PMD2.G and psPAX2 were kindly gifted by Professor Rui Luo (Wuhan, China). Lenti-CRISPR-sgRNA-V2-Puro was gifted by Professor Shengsong Xie (Wuhan, China). SgRNAs were designed according to a library of Genome-scale CRISPR knock-out, and were cloned into the Lenti-CRISPR-sgRNA-V2-Puro vector. Swine *IRF3*, *MAVS*, *TBK1*, *IKK* gene was cloned into eukaryotic expression vector pCAGGS-HA. Primers used for genes amplifications are shown in Table S1 in Supporting Information.

RNA isolation and qRT-PCR

For qRT-PCR, cells were lysed with TRIzol reagent (Invitrogen, USA), and total RNA was extracted according to the manufacturer's instructions. One to two micrograms of RNA was used to generate cDNA using reverse transcriptase (ABclonal Biotechnology). Real-time PCR (ABI, USA) was performed using FastStart Universal SYBR green (ABclonal Biotechnology). The PCR conditions were 2 min at 50°C, 10 min at 95°C, and then 40 cycles for 15 s at 95°C and 30 s at 60°C. GAPDH was used as a control for the normalization of cellular mRNA. Primers used for qRT-PCR are shown in Table S2 in Supporting Information.

Generation of the BEND6 KO PK-15 cells

The single-guide RNA (sgRNA) sequence targeting the swine BEND6 gene (5′-CACCGAGAGAACGTCAACAGTGACG-3′) was cloned into Lenti-CRISPR-sgRNA-V2-Puro vector to produce the recombined lentivirus. The PK-15 cells were infected with the BEND6 Lenti-CRISPR-sgRNA-V2-Puro lentivirus, and puromycin (2.5 μg mL^{-1}) was added to select the positive cells at 24 hpi. The monoclonal cells were acquired by using the limiting dilution method in 96-well plates. Finally, the BEND6-KO cells were obtained from these enlarged monoclonal cells and confirmed by western blot and Sanger sequencing.

Cell viability assay

The proliferation ability of cells after knockout was measured by CCK-8 activity according to the manufacturer's instructions (GLPBIO, USA). Briefly, BEND6 KO and WT PK-15 cells were seeded at equal densities in 96-well plates. The cell viability was detected after 12, 24, and 36 h, when cell density reached 50% CCK-8 reagent was added to each well of plate, and the absorbance at 450 nm was measured by a microplate reader after 1 h of incubation.

Virus titration

Viral supernatants were titrated on MDCK cells. Briefly, the serially diluted supernatants were inoculated onto MDCK cell monolayers in 96-well plates for 1 h, and the inoculum was removed and replaced with DMEM containing 0.25 μg mL^{-1} of Trypsin-TPCK (Sigma, USA). The plates were incubated for 72 h at 37°C. Virus titers were determined by calculating $\log_{10}$ 50% tissue culture infectious dose (TCID50)/milliliter using the Reed-Muench method.

Dual luciferase activity assay

HEK293T cells in 12-well plates were transfected with the internal control pRL-TK, IFN-β-luc or ISRE-luc. To stimulate promoter activity, cells were co-transfected with the swine RIG-I, MAVS, TBK1, IKK, and IRF3 expression plasmids, or infected with Sev at 24 h post-transfection. At 24 h post-transfection or 12 h postinfection, cells were lysed in 300 μL of 1× passive lysis buffer (Promega, USA). The luciferase activity and Renilla activity were measured using a dual-luciferase assay kit (Promega) according to the manufacturer's instructions. Renilla luciferase activity was used as an internal control and to normalize transfection efficiency. All experiments were performed in triplicate and repeated at least three times.

Immunofluorescence and confocal microscopy

WT PK15 cells or BEND6 KO cells were seeded in confocal dish. The cells were fixed with 4% paraformaldehyde for 15 min, permeabilized with 0.2% Triton X-100 (Sigma-Aldrich, USA) in phosphate buffer saline (PBS) for 10 min, and blocked with 4% bovine serum albumin (BSA) for 1 h at room temperature. Subsequently, the cells were incubated with the corresponding primary antibodies overnight at 4°C. Subsequently, the cells were incubated in 594-conjugated goat anti-mouse secondary antibody for 1 h. Nuclei were stained with DAPI (Invitrogen) for 10 min. After each step, cells were washed five times with PBS. Images were acquired with a confocal microscope (Carl Zeiss LSM 880 Confocal Microscope and ZEN 2.3 LITE software).

CO-IP and western blot assay

HEK293T cells seeded in 10-cm dishes were transfected in 10 μg of the indicated expression plasmids by using Lipofectamine 2000 (Invitrogen). Subsequently, at 36 h post-transfection, cells were lysed with immunoprecipitation (IP) lysis buffer (Beyotime, Shanghai, China) together with a protease inhibitor cocktail (BioTools, USA) on ice, and then the lysis was centrifuged. Supernatants were collected and incubated with anti-HA immunomagnetic beads (Bimake, USA) or anti-Flag immunomagnetic beads (Bimake) overnight at 4°C. For endogenous IP, the cell lysates were incubated with beads conjugated with IGg or BEND6 mouse anti-body at 4°C overnight. The beads were washed five times with cold IP lysis buffer and were eluted with 5× loading buffer by boiling of samples for 10 min before western blot analysis. Images were obtained using an ECL detection system (Tanon, Shanghai, China).

DNA pulldown assay

DNA probes were synthesized by Tsingke Biological Technology (Wuhan, China). The sequences of triple repeats of the ISG54 ISRE (5′-GGGAAAGTGAAACTAGGGAAAGTGAAACTAGGGAAAGTGAAACTA-3′) (Meng et al., 2016; Nakaya et al., 2001), which can be recognized and bound by the activated swine IRF3, were labeled with biotin and used in the pulldown experiments. An unbiotinylated ISRE was used to compete away IRF3-BEND6 or BEND6 binding. Single strains of DNA were thermally annealed to form dsDNA prior to pulldown experiments. HEK293T cells transfected with the indicated plasmids were infected with SeV. At 12 hpi, cells were lysed, and the lysates were then mixed with DNA probes and incubated for 4 h at 4°C. For BEND6 binding experiments, 10 μg equal amounts of BEND6-His protein and 4M2e-His protein were mixed with DNA probes and incubated for 4 h at 4°C. The streptavidin beads (Beaver, Suzhou, China) were washed three times with the buffer (10 mmol L^{-1} Tris-HCl, 1 mmol L^{-1} EDTA, 1 mol L^{-1} NaCl, 0.01% to 0.1% (vol/vol) Tween 20, pH 7.5) and then added to the lysates for 2 h of incubation at 4°C. The beads were collected by magnetic separator and washed four times with cold PBS. Finally, the beads were resuspended in 1× SDS loading buffer, and bound proteins were resolved by SDS-PAGE, followed by immunoblotting with Flag-antibody.

ELISA

Microtiter plates (BIOFIL, Guangzhou, China) were coated with 100 μL of BEND6-His proteins at a concentration of 4 μg mL^{-1} in PBS and incubated overnight at 4°C. Following three washes with PBST (PBS with 0.05% Tween), the plates were blocked with 5% non-fat milk (BD, USA) in PBS for 2 h at 37°C. Subsequently, the plates were washed three times and 100 μL of the anti-BEND6 or negative antibody was added to each well, followed by incubation for 1 h at 37°C. After three additional washes, 100 μL of HRP-goat anti-porcine IgG (H+L) (1:3,000) (SouthernBiotech, USA) was added to each well and incubated for 30 min at 37°C. Following extensive washing, TMB Chromogenic Solution (50 μL of A and 50 μL of B) (Keqian Biology, Wuhan, China) was added to each well and incubated for 10 min at room temperature. The reaction was terminated by adding 50 μL of 2 mol L^{-1} H_2SO_4. The optical density (OD) value at 630 nm was measured using a microplate reader (PerkinElmer, USA).

Statistical analyses

Data were presented as means±standard deviations (SD). Statistical analysis was performed by a paired two-tailed Student's *t* test. *P* value equal or lower to 0.05 was considered significant (**P*<0.05, ***P*<0.01, ****P*<0.001). *P* value>0.05 was considered statistically non-significant.

Compliance and ethics

The authors declare that they have no conflict of interest.

Acknowledgement

This work was supported by the National Key Research and Development Program of China (2021YFD1800204), the National Natural Science Foundation of China (32025036), the Fundamental Research Funds for the Central Universities (2662023PY005), Hubei Hongshan Laboratory (2022hszd005), the earmarked fund for CARS-41 and the Natural Science Foundation of Hubei Province (2021CFA016). We thank Xiao Xiao (Huazhong Agricultural University, Wuhan, China) for critically proofreading the manuscript. We acknowledge the support of the National Key Laboratory of Agricultural Microbiology Core Facility for their aid in confocal microscopy.

Supporting information

The supporting information is available online at https://doi.org/10.1007/s11427-024-2698-6. The supporting materials are published as submitted, without typesetting or editing. The responsibility for scientific accuracy and content remains entirely with the authors.

References

Abhiman, S., Iyer, L.M., and Aravind, L. (2008). BEN: a novel domain in chromatin factors and DNA viral proteins. Bioinformatics 24, 458–461.

Akiyama, H., Ramirez, N.G.P., Gibson, G., Kline, C., Watkins, S., Ambrose, Z., Gummuluru, S., and Kirchhoff, F. (2017). Interferon-inducible CD169/Siglec1 attenuates anti-HIV-1 effects of alpha interferon. J Virol 91, e00972–17.

Bussey, K.A., Lau, U., Schumann, S., Gallo, A., Osbelt, L., Stempel, M., Arnold, C.,

Wissing, J., Gad, H.H., Hartmann, R., et al. (2018). The interferon-stimulated gene product oligoadenylate synthetase-like protein enhances replication of Kaposi's sarcoma-associated herpesvirus (KSHV) and interacts with the KSHV ORF20 protein. PLoS Pathog 14, e1006937.
Das, A., Barrientos, R., Shiota, T., Madigan, V., Misumi, I., McKnight, K.L., Sun, L., Li, Z., Meganck, R.M., Li, Y., et al. (2020). Gangliosides are essential endosomal receptors for quasi-enveloped and naked hepatitis A virus. Nat Microbiol 5, 1069–1078.
Duan, H., Dai, Q., Kavaler, J., Bejarano, F., Medranda, G., Nègre, N., and Lai, E.C. (2011). Insensitive is a corepressor for Suppressor of Hairless and regulates Notch signalling during neural development. EMBO J 30, 3120–3133.
Fairman, C.W., Lever, A.M.L., and Kenyon, J.C. (2021). Evaluating RNA structural flexibility: viruses lead the way. Viruses 13, 2130.
Fitzgerald, K.A., McWhirter, S.M., Faia, K.L., Rowe, D.C., Latz, E., Golenbock, D.T., Coyle, A.J., Liao, S.M., and Maniatis, T. (2003). IKKε and TBK1 are essential components of the IRF3 signaling pathway. Nat Immunol 4, 491–496.
Gélinas, J.F., Clerzius, G., Shaw, E., and Gatignol, A. (2011). Enhancement of replication of RNA viruses by ADAR1 via RNA editing and inhibition of RNA-activated protein kinase. J Virol 85, 8460–8466.
Kell, A.M., and Gale Jr., M. (2015). RIG-I in RNA virus recognition. Virology 479-480, 110–121.
Lai, J.H., Wu, D.W., Wu, C.H., Hung, L.F., Huang, C.Y., Ka, S.M., Chen, A., and Ho, L. J. (2023). USP18 enhances dengue virus replication by regulating mitochondrial DNA release. Sci Rep 13, 20126.
Liu, K., Zhang, J., Xiao, Y., Yang, A., Song, X., Li, Y., Chen, Y., Hughes, T.R., and Min, J. (2023). Structural insights into DNA recognition by the BEN domain of the transcription factor BANP. J Biol Chem 299, 104734.
McWhirter, S.M., Fitzgerald, K.A., Rosains, J., Rowe, D.C., Golenbock, D.T., and Maniatis, T. (2004). IFN-regulatory factor 3-dependent gene expression is defective in *Tbk1*-deficient mouse embryonic fibroblasts. Proc Natl Acad Sci USA 101, 233–238.
Meng, F., Zhou, R., Wu, S., Zhang, Q., Jin, Q., Zhou, Y., Plouffe, S.W., Liu, S., Song, H., Xia, Z., et al. (2016). Mst1 shuts off cytosolic antiviral defense through IRF3 phosphorylation. Genes Dev 30, 1086–1100.
Nakagawa, S., Sakaguchi, S., Ogura, A., Mineta, K., Endo, T., Suzuki, Y., and Gojobori, T. (2023). Current trends in RNA virus detection through metatranscriptome sequencing data. FEBS Open Bio 13, 992–1000.
Nakaya, T., Sato, M., Hata, N., Asagiri, M., Suemori, H., Noguchi, S., Tanaka, N., and Taniguchi, T. (2001). Gene induction pathways mediated by distinct IRFs during viral infection. Biochem Biophys Res Commun 283, 1150–1156.
Rivera, A., Siracusa, M.C., Yap, G.S., and Gause, W.C. (2016). Innate cell communication kick-starts pathogen-specific immunity. Nat Immunol 17, 356–363.
Sharma, S., tenOever, B.R., Grandvaux, N., Zhou, G.P., Lin, R., and Hiscott, J. (2003). Triggering the interferon antiviral response through an IKK-related pathway. Science 300, 1148–1151.
Wang, H., Chao, S., Yan, Q., Zhang, S., Chen, G., Mao, C., Hu, Y., Yu, F., Wang, S., Lv, L., et al. (2024). Genetic diversity of RNA viruses infecting invertebrate pests of rice. Sci China Life Sci 67, 175–187.
Wang, J., and Chai, J. (2020). Molecular actions of NLR immune receptors in plants and animals. Sci China Life Sci 63, 1303–1316.
Wang, Z., Wu, T., Ma, M., Zhang, Z., Fu, Y., Liu, J., Xu, J., Ding, H., Han, X., Chu, Z., et al. (2017). Elevated interferon-γ–induced protein 10 and its receptor CXCR3 impair NK cell function during HIV infection. J Leukoc Biol 102, 163–170.
Weaver, B.K., Kumar, K.P., and Reich, N.C. (1998). Interferon regulatory factor 3 and CREB-binding protein/p300 are subunits of double-stranded RNA-activated transcription factor DRAF1. Mol Cell Biol 18, 1359–1368.
Wei, J., Alfajaro, M.M., DeWeirdt, P.C., Hanna, R.E., Lu-Culligan, W.J., Cai, W.L., Strine, M.S., Zhang, S.M., Graziano, V.R., Schmitz, C.O., et al. (2021). Genome-wide CRISPR screens reveal host factors critical for SARS-CoV-2 infection. Cell 184, 76–91.e13.
Wu, K., Oberstein, A., Wang, W., and Shenk, T. (2018). Role of PDGF receptor-α during human cytomegalovirus entry into fibroblasts. Proc Natl Acad Sci USA 115, E9889–E9898.
Yang, C., Liu, X., Cheng, T., Xiao, R., Gao, Q., Ming, F., Jin, M., Chen, H., Zhou, H., and Williams, B.R.G. (2019). LYAR suppresses beta interferon induction by targeting phosphorylated interferon regulatory factor 3. J Virol 93, e00769-19.
Yu, J., Liang, C., and Liu, S.L. (2017). Interferon-inducible LY6E protein promotes HIV-1 infection. J Biol Chem 292, 4674–4685.
Zhang, Y.Y., Chen, Y., Wei, X., and Cui, J. (2022). Viromes in marine ecosystems reveal remarkable invertebrate RNA virus diversity. Sci China Life Sci 65, 426–437.
Zhu, T., Niu, G., Zhang, Y., Chen, M., Li, C.Y., Hao, L., and Zhang, Z. (2023). Host-mediated RNA editing in viruses. Biol Direct 18, 12.